The Astrophysical Journal, 941:179 (8pp), 2022 December 20 https://doi.org/10.3847/1538-4357/aca40c

Searching for Candidates of Coalescing Binary Black Holes Formed through Chemically Homogeneous Evolution in GWTC-3

Ying Qin[1], Yuan-Zhu Wang[2], Simone S. Bavera[3,4], Shichao Wu[5,6], Georges Meynet[3,4], Yi-Ying Wang[7,8], Rui-Chong Hu[9], Jin-Ping Zhu[10], Dong-Hong Wu[1], Xin-Wen Shu[1], Fang-Kun Peng[1], Han-Feng Song[11], and Da-Ming Wei[7,8]

[1] Department of Physics, Anhui Normal University, Wuhu, Anhui 241000, People's Republic of China; wangyz@pmo.ac.cn
[2] Key Laboratory of Dark Matter and Space Astronomy, Purple Mountain Observatory, Chinese Academy of Sciences, Nanjing, 210033, People's Republic of China; Simone.Bavera@unige.ch
[3] Département dAstronomie, Université de Genève, Chemin Pegasi 51, CH-1290 Versoix, Switzerland; yingqin2013@hotmail.com
[4] Gravitational Wave Science Center (GWSC), Université de Genève, CH-1211 Geneva, Switzerland
[5] Max-Planck-Institut für Gravitationsphysik (Albert-Einstein-Institut), D-30167 Hannover, Germany
[6] Leibniz Universität Hannover, D-30167 Hannover, Germany
[7] Key Laboratory of Dark Matter and Space Astronomy, Purple Mountain Observatory, Chinese Academy of Sciences, Nanjing, 210033, People's Republic of China
[8] School of Astronomy and Space Science, University of Science and Technology of China, Hefei, Anhui 230026, People's Republic of China
[9] Guangxi Key Laboratory for Relativistic Astrophysics, School of Physical Science and Technology, Guangxi University, Nanning 530004, People's Republic of China
[10] Department of Astronomy, School of Physics, Peking University, Beijing 100871, People's Republic of China
[11] College of Physics, Guizhou University, Guiyang city, Guizhou Province, 550025, People's Republic of China
Received 2022 February 7; revised 2022 November 7; accepted 2022 November 10; published 2022 December 22

Abstract

The LIGO, Virgo, and KAGRA (LVK) Collaboration has announced 90 coalescing binary black holes (BBHs) with $p_{\rm astro} > 50\%$ to date; however, the origin of their formation channels is still an open scientific question. Given various properties of BBHs (BH component masses and individual spins) inferred using the default priors by the LVK, independent groups have been trying to explain the formation of the BBHs with different formation channels. Of all formation scenarios, the chemically homogeneous evolution (CHE) channel has stood out with distinguishing features, namely, nearly equal component masses and preferentially high individual spins aligned with the orbital angular momentum. We perform Bayesian inference on the BBH events officially reported in GWTC-3 with astrophysically predicted priors representing different formation channels of the isolated binary evolution (common-envelope evolution channel, CEE; CHE; stable mass transfer, SMT). Given assumed models, we report strong evidence for GW190517_055101 being most likely to have formed through the CHE channel. Assuming the BBH events in the subsample are all formed through one of the isolated binary evolution channels, we obtain the lower limits on the local merger rate density of these channels at 11.45 $\rm Gpc^{-3}\,yr^{-1}$ (CEE), 0.18 $\rm Gpc^{-3}\,yr^{-1}$ (CHE), and 0.63 $\rm Gpc^{-3}\,yr^{-1}$ (SMT) at 90% credible level.

Unified Astronomy Thesaurus concepts: Gravitational wave sources (677); Stellar mass black holes (1611); Close binary stars (254)

1. Introduction

To date, a total of 90 merging binary black holes (BBHs) with $p_{\rm astro}$ of at least 50%, have been reported in the third LIGO, Virgo, and KAGRA (LVK) Collaboration Gravitational-Wave Transient Catalog (GWTC-3; Abbott et al. 2020b, 2021a). GW190517_055101, first reported in GWTC-2 (Abbott et al. 2021c) with $p_{\rm astro} > 0.99$, has a primary BH mass $M_1 = 37.4^{+11.7}_{-7.6} M_\odot$ and a secondary BH mass $M_2 = 25.5^{+7.0}_{-7.3} M_\odot$ (mass ratio $q = M_2/M_1 \sim 0.68$) at the 90% credible level. This event has stood out with the highest effective spin in GWTC-3[12] ($\chi_{\rm eff} = 0.52^{+0.19}_{-0.19}$). At the leading post-Newtonian order, the gravitational wave signals are largely dependent on the effective spin parameter $\chi_{\rm eff}$ (Damour 2001), which is defined as:

$$\chi_{\rm eff} = \frac{(M_1 \boldsymbol{\chi}_1 + M_2 \boldsymbol{\chi}_2) \cdot \hat{L}}{M_1 + M_2}, \quad (1)$$

where M_1 and M_2 are the component masses, $\boldsymbol{\chi}_1$ and $\boldsymbol{\chi}_2$ are their corresponding dimensionless spin parameters, and $\hat{L}$ is the unit vector along the orbital angular momentum (AM).

Various formation channels of BBHs (see recent reviews of Mapelli 2021; Mandel & Farmer 2022) have been proposed since the first discovery of gravitational waves, GW150914 (Abbott et al. 2016b). The leading formation channels can be divided into two broad categories, i.e., isolated binary evolution and dynamical formation. The former category includes (i) the classic isolated binary evolution scenario involving a common-envelope evolution phase (CEE channel, e.g., Tutukov & Yungelson 1993; Lipunov et al. 1997; Bethe & Brown 1998; Belczynski et al. 2002, 2016; Kalogera et al. 2007; Bavera et al. 2020; Zevin & Bavera 2022); (ii) a double stable mass-transfer phase (SMT channel, e.g., Inayoshi et al. 2017; van den Heuvel et al. 2017; Neijssel et al. 2019; Bavera et al. 2021, 2022b; Olejak & Belczynski 2021), or both stars evolving chemically homogeneously (CHE channel, e.g., Marchant et al. 2016;

[12] Note that GW190403_051519 has a lower $p_{\rm astro}$ ($p_{\rm astro} > 50\%$), although it was reported with the $\chi_{\rm eff} = 0.70^{+0.15}_{-0.27}$.

Mandel & de Mink 2016; de Mink & Mandel 2016; du Buisson et al. 2020; Zevin et al. 2021; Riley et al. 2021; Bavera et al. 2022c). Dynamical formation in dense stellar environments includes formation in globular clusters, young stellar clusters, and open stellar clusters (e.g., Rodriguez et al. 2015; Fragione & Kocsis 2018), active galactic nuclei disks (McKernan et al. 2018; Tagawa et al. 2020), and isolated triple or higher-order stellar systems (e.g., Silsbee & Tremaine 2017; Rodriguez & Antonini 2018; Toonen et al. 2020; Gupta et al. 2020).

In general, the effective spin $\chi_{\rm eff}$ has been widely regarded as a discriminator for disentangling the isolated (individual BH spins preferentially aligned to the direction of the orbital AM) and dynamical (random orientations of individual BH spins) formation scenarios (Rodriguez et al. 2016; Farr et al. 2017, 2018; Stevenson et al. 2017; Talbot & Thrane 2017; Vitale et al. 2017). Of all the formation channels mentioned above, the CHE channel has been considered as the most likely scenario that can lead to the formation of BBH systems with: (i) nearly equal masses (Marchant et al. 2016; Mandel & de Mink 2016); (ii) two BHs with preferentially high spins that are aligned to the orbital AM (Marchant et al. 2016; du Buisson et al. 2020; Zevin et al. 2021; Bavera et al. 2022c). Therefore, these two features can be used as a probe to investigate whether or not there is quantitative high-confidence evidence of any merging BBHs formed through the CHE channel. Recent studies (Galaudage et al. 2021; Roulet et al. 2021; Vitale et al. 2022) have pointed out that the inferred spin and mass parameters are dependent on the choice of priors.[13] This is because the measurements of spin and mass are poorly constrained, and so the resulting broad posteriors can be heavily swayed by one's choice of prior. In particular, some specific events have also been recently reanalyzed with different priors than the official LVK analysis. Assuming as a prior that the more massive BH has a zero spin and that the rotation axis of the less massive BH is aligned with the orbital AM, Mandel & Fragos (2020) argued that, in the context of isolated binary evolution, the less massive component of GW190412 could be highly spinning. Zevin et al. (2020) further investigated how the choice of a prior can influence parameter estimates of GW190412. Mandel & Smith (2021) suggested that a prior of nonspinning BH for GW200115 is more consistent with current astrophysical understanding. Fishbach & Holz (2020) pointed out that GW190521 likely straddles the pair-instability gap by reanalyzing its signal with a population-informed prior on less massive BH mass. These findings confirm that the choice of a prior can play a critical role in inferring the properties of gravitational-wave sources.

Different groups have independently investigated the formation channels of observed BBHs (e.g., Bouffanais et al. 2021; Wong et al. 2021, 2022; Franciolini et al. 2022; Mapelli et al. 2022). Recently, Zevin et al. (2021) found that multiple channels are required when interpreting the currently released LVK's BBHs, assuming a limited number of model uncertainties and a subsample of all possible formation scenarios. In their models that are publicly available, the predictions for spin and mass distributions have been presented for various astrophysical formation channels of BBHs. In this work, we perform Bayesian inference to search for evidence of BBHs most likely formed through the CHE channel by considering the models of isolated binary evolution CEE/SMT/CHE of Bavera et al. (2021) and du Buisson et al. (2020) (as released by Zevin 2021) as the astrophysically predicted priors. In Section 2, we first briefly introduce the CHE and its predicted properties of BBHs. Then we present our Bayesian analysis and results in Section 3. Finally, the main conclusions and some discussion are summarized in Section 4.

2. Properties of BBHs Predicted by the CHE Channel

Chemical mixing induced by fast rotation leads to massive stars evolving homogeneously, without expanding to become a red supergiant star (Maeder 1987). Martins et al. (2013) performed a spectroscopic analysis of Wolf–Rayet stars in the Large Magellanic Cloud and the Milky Way, and found that some of these objects might have gone through the CHE. In order to sustain efficient mixing throughout their lifetimes, single massive stars must be rotating quickly at birth, requiring metal-poor environments, where the stellar winds are weak (Vink et al. 2001). For massive stars that can be efficiently spun up by the tidal interaction in close binaries at subsolar metallicities, rotationally enhanced mixing has been predicted to produce the CHE for both stars (Song et al. 2016; Marchant et al. 2016; Mandel & de Mink 2016) or only the more massive component (de Mink et al. 2009; Marchant et al. 2017; Qin et al. 2019). Observations for the O-type stars in six nearby Galactic open stellar clusters show that ∼70% of O-type stars are in close binaries and about 1/3 of them are able to interact on the main sequence (Sana et al. 2012). Furthermore, de Mink et al. (2013) simulated a massive binary-star population to find that the rapid rotation of massive stars could be obtained via mass transfer or mergers. Alternatively, the CHE induced by the accretion from its companion could also be reached for massive stars with weak tidal interactions in relatively wide orbits (Cantiello et al. 2007). Recently, Ghodla et al. (2023) claimed that the accretion-induced CHE could be an important formation channel producing electromagnetic transients like GRBs/Ic-BL (SLSN-I/Ic-BL)[14] under the collapsar (magnetar) scenario. In addition to CEE and SMT, the CHE was also found to play a critical role in contributing to the long GRB rate (Bavera et al. 2022c).

Massive stars with nearly equal masses in close binaries tend to follow the CHE and thus result in binary BHs that could merge within a Hubble time (Marchant et al. 2016; Mandel & de Mink 2016; de Mink & Mandel 2016; du Buisson et al. 2020; Zevin et al. 2021; Riley et al. 2021; Bavera et al. 2022a, 2022c). Treatments of CHE and predictions of its outcome have been calculated by a variety of techniques, ranging from simplified prescriptions (e.g., Mandel & de Mink 2016; Riley et al. 2021) to detailed models of massive binary evolution (Marchant et al. 2016; du Buisson et al. 2020). As mentioned earlier, current models predict that BBHs formed through the CHE are expected to have mass ratios close to unity and preferentially high inspiral effective spins $\chi_{\rm eff}$. First, Mandel & de Mink (2016) showed that there is a strong preference for two BHs with comparable masses, and especially that there are no BH binaries of interest with the mass ratio $q < 0.5$. Therefore, the mass ratio $q = 0.5$ can be used as a lower limit for forming merging BBHs through the CHE channel. Additionally, Marchant et al. (2016) and du Buisson et al. (2020) found that BBHs originated from the

[13] Prior: probability distribution that represents knowledge or uncertainty of a data object before observing it.

[14] GRB: gamma-ray burst; Ic-BL: broad-lined type Ic supernova; SLSN: superluminous supernova type I.

CHE tend to have mass ratio $q > 0.8$. Second, as expected for BBHs formed through CHE, high BH spins can be reached (see Figure 9 in Marchant et al. 2016). We would expect even higher effective spins $\chi_{\rm eff}$ for BBHs formed through the CHE if less efficient AM transport within their progenitors is assumed (e.g., see the green line for $\chi_{\rm eff}$ in the bottom panels of Figure 1 in Zevin et al. 2021).

Olejak & Belczynski (2021) used population synthesis models to find that, two equal-mass helium stars might be formed after the CE phase and then produce two fast-spinning BHs with the mass ratio $q = 1$. Such double helium-star systems, however, are more common to be produced through the CHE channel (see Figure 3 for a parameter-space study of detailed binary calculations in Marchant et al. 2016), which most likely produce two equal-mass BHs. Therefore, in this work, we consider the BBHs with equal masses to be more likely formed through the CHE channel. For BBHs formed via the SMT channel, the orbital separation after the second mass-transfer phase is much wider when compared with CEE. Therefore, the $\chi_{\rm eff}$ was expected to be very low, i.e., $\chi_{\rm eff} < 0.1$ (see Figure 2 in Bavera et al. 2021), assuming the accretion onto BHs is Eddington limited.[15] For the channel of the CEE (see detailed investigations of this channel in Bavera et al. 2020), it has been recently shown in Qin et al. (2022b) that the upper limit of $\chi_{\rm eff}$ is constrained to not be higher than 0.5, assuming that the first-born BH is formed from an initially more massive star with a strongly efficient AM transport mechanism (i.e., the revised version of original Tayler–Spruit dynamo in Fuller et al. 2019; see similar results that were also yielded in Qin et al. 2018, Belczynski et al. 2020, and Fuller & Lu 2022 for a recent investigation[16]).

It is important to note that identifying events from different channels requires a solid understanding of the predictions of these channels. To date, the predictions for the different channels are plagued due to major uncertainties (e.g., Belczynski et al. 2022; Broekgaarden et al. 2022). In this work, we are focused on searching for possible candidates that could have very similar properties predicted by the CHE channel under our current understanding of its relevant physical processes.

3. Analysis and Results

We perform Bayesian inference on the BBH events with various priors representing different formation channels of the isolated binary evolution (CEE, CHE, and SMT). Figure 1 shows the model predictions (we refer interested readers to the detailed descriptions in Zevin et al. 2021) on the marginal distributions of chirp mass $\mathcal{M}_{\rm c}$[17], mass ratio q, and component spins (χ_1, χ_2) of different BBH formation channels of the isolated binary evolution. Ideally, one should use the joint distributions ($p(\mathcal{M}_{\rm c}, q, \chi_1, \chi_2)$) as priors in the inference to preserve the potential correlations as predicted by the models. However, it is numerically difficult to approximate the 4D probability distribution function (PDF) with a kernel density estimation, so for simplicity we adopt 1D marginal distributions as priors in this study. For the CHE channel, we extend the lower limit of the mass ratio q down to 0.5 (0.8 adopted in Zevin et al. 2021; see Figure 1) to be consistent with the predictions of Mandel & de Mink (2016), assuming the same spin values ($\chi_1 = \chi_2$) for the two BHs formed through the CHE channel;

We carry out a preliminary selection for the potential candidates being formed through CHE. The events listed in Table 1 are candidates that pass our selection criteria. They have properties (inferred by the LVK's default prior) that satisfied (i) $\mathcal{M}_{\rm c,M} < 40\,M_\odot$; (ii) $q_M > 0.5$; (iii) $\chi_{1{\rm z},M} > 0.05$, where the subscribe "M" represents the median value of the posterior samples.

The Bayesian inference takes the strain data of an event, the waveform model, the power spectral density, and the prior for the parameters representing the binary's properties as input, and returns the parameters' posterior distributions as output. One can derive the Bayes factor, $\mathcal{B}$, between two models (waveform + prior) by comparing the Bayesian evidence $\mathcal{E}$ (Thrane & Talbot 2019; Zevin et al. 2020). The Bayes factor reflects a comprehensive evaluation of the goodness-of-fit and the prior volume for the two models. Therefore, the larger the Bayes factor, the more favored the formation channel indicated.

We choose the source frame chirp mass $\mathcal{M}_{\rm c}$, the mass ratio q, the individual BH spin magnitude χ_i, and the tilt angle of component spin θ_i to describe the intrinsic properties of the BBHs in the sampling. Although several individual BBHs have been identified as possibly exhibiting precessional effects due to spin misalignment (Abbott et al. 2020; Islam et al. 2021; Estellés et al. 2022; Chia et al. 2022; Hoy et al. 2022; Payne et al. 2022; Vajpeyi et al. 2022) such evidence for individual-event precessional has generally been weak or inconclusive. In this study, since BH spins are expected to be aligned with the orbital AM vector in the CHE channel, we adopt $\theta_i = 0$ in our inference by assuming aligned spins in all of our samples. To increase the efficiency of the parameter estimation process, we also make a simplification of the priors of χ_1: we fix $\chi_1 = 0$ for the CEE and SMT channels, since for these two channels we assume all first-born BHs have negligible $\chi_{1{\rm z}}$ ($\chi_{1{\rm z}} < 0.01$) as shown in Figure 1.

We use the publicly available data for the selected events from the Gravitational Wave Open Science Center[18], and adopt a duration of 17 s covering the detection time in the analysis. The results are produced using the python package *bilby* (Ashton et al. 2019) and its built-in sampler *dynesty* (Speagle 2020). The low and high frequency cutoffs for the likelihood calculation are set to 20 (30) Hz and 512 Hz, respectively, for LIGO (Virgo) detectors. We employ the Phenom waveform family in the inference, and choose the model IMRPhenomXP (Pratten et al. 2021) since it achieves a good trade-off between accuracy and speed.

The resulting Bayes factors of the CHE prior as well as the SMT prior compared to the CEE prior are listed in the brackets in Table 1. In addition to $\mathcal{B}$, we also consider the theoretical predictions of the merger rate density in the local universe ($z = 0$) of each channel as prior odds to compute the odds ratio ($\mathcal{O}$): $\mathcal{O} = \mathcal{B} \times (\mathcal{R}_i/\mathcal{R}_{\rm CEE})$, where $\mathcal{R}_i/\mathcal{R}_{\rm CEE}$ is the relative rate of a specific channel with respect to the CEE channel. We adopt the predictions in Bavera et al. (2022c), showing the CEE, CHE, and SMT channel would contribute to 29%, 14%,

[15] BHs can be efficiently spun up in binaries if one assumes that hypercritical accretion Qin et al. (2022a) or mildly super-Eddington accretion (Shao & Li 2022) is allowed.

[16] The spins of BHs born from single stars have been predicted to be small ($\chi \lesssim 0.01$, Qin et al. 2018; Fuller & Ma 2019, and $\chi \sim 0.1$, Belczynski et al. 2020).

[17] $\mathcal{M}_{\rm c} = \frac{(M_1 M_2)^{3/5}}{(M_1+M_2)^{1/5}}$, where M_1 and M_2 are the masses of the two BHs, respectively.

[18] https://www.gw-openscience.org/eventapi/html

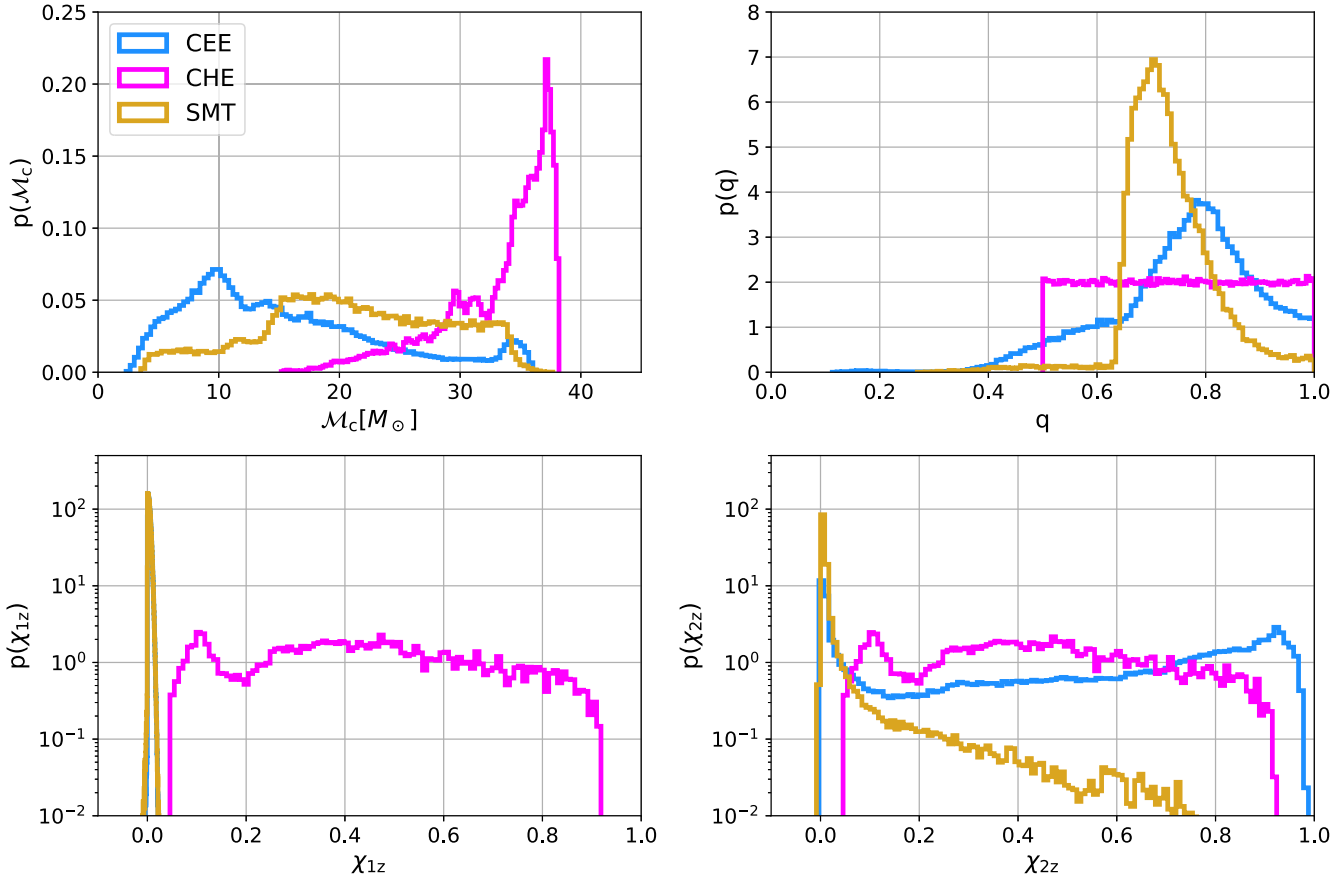

Figure 1. Theoretical predictions of the marginal distributions (blue: CEE; magenta: CHE; green: SMT) of chirp mass ($\mathcal{M}_c$), mass ratio (q), and component spins ($\chi_{1z} = \chi_1$, $\chi_{2z} = \chi_2$, assuming both χ_{1z} and χ_{1z} are aligned to the direction of the orbital AM). The simulated data are obtained from the publicly released models in Zevin et al. (2021), except that for the CHE channel we extend the q distribution down to 0.5, which is in agreement with the studies in Mandel & de Mink (2016) and de Mink & Mandel (2016).

and 57% of the events originated from isolated binary evolution. The adopted mixing fractions are consistent with the models used in Zevin et al. (2021). In practice these values might change due to model uncertainties (Mandel & Broekgaarden 2022). We use the odds ratio as the final indicator to determine the preference for formation channels. If $\mathcal{O}$ is larger than 3/30/100 (Abbott et al. 2021d), one can conclude that a moderate/strong/very strong evidence of preference is found for a prior over the CEE prior. On the other hand, if $1/3 < \mathcal{O} < 3$, the priors have comparable support from the data. In Table 1, we find that six out of 26 events have $\mathcal{O} > 1/3$ ($\ln \mathcal{O} > -1.1$) for the CHE prior, while 14 events have $\mathcal{O} > 1/3$ for the SMT prior. We also note that several events show a strong favor for the CEE prior (see the bottom in Table 1). This result could be explained by adopting combined priors of chirp mass, mass ratio, and two spin components, especially for $\chi_{1z} \sim 0$ and a more broad distribution of χ_{2z} (i.e., from 0 to 1).

Most notably, for the CHE prior, GW190517_055101 has the largest $\mathcal{O}$ of $\ln \mathcal{O} = 3.4$ ($\mathcal{O} = 30$), which is at the threshold of being strong evidence for the preference of the CHE prior against the CEE prior. These results may be due to the fact that the CHE prior allows for much larger individual spins when compared with the CEE and SMT channels, which is needed to better match the gravitational waveform for this event; in addition, the 1D chirp mass prior for the CHE channel has larger probability densities around the inferred chirp mass $\sim 28\ M_\odot$. In contrast, the logarithmic $\mathcal{O}$ for the SMT prior is -8.7, indicating that this prior is much less supported than the others. Additionally, the finding also indicates that the CEE prior is not favored. This is most likely due to the lower χ_{1z} predicted by the two channels (CHE and SMT). Assuming BBHs originated from isolated binary evolution and given the considered models, our analysis favors the CHE origin of GW190517_055101. In Figure 2, we show the properties of this event inferred by LVK's default prior (Abbott et al. 2021c), and the result inferred with our CHE prior (magenta) for comparison. Under the default prior, both BH individual spins have most of their posterior supports at $\chi_i \sim 1$ (though χ_2 is barely constrained). The marginal mass ratio distribution peaks at $q \sim 0.6$, and there is still posterior supports at $q = 1$. Despite a nearly identical constraint on the chirp mass, using our CHE prior yields different posteriors for q, χ_1, and χ_2. The individual spin distributions peak at $\chi_i \sim 0.5$; extreme values ($\chi_i \sim 0$ and $\chi_i \sim 1$) for the spins are also excluded. The peak of the mass ratio distribution shifts to $q \sim 0.9$, and the distribution has a low probability density at the lower edge (0.5) of the mass ratio prior. Callister et al. (2021) recently showed that the mass ratio of GW190517_055101 under a population-informed prior can be relatively low (down to ~ 0.25) assuming it follows the $\chi_{\rm eff}$–q anticorrelation, which was also corroborated by Adamcewicz & Thrane (2022) using a different statistical approach. This confirms that different prior assumptions may lead to diverse results and the CHE prior in this work provides an alternative solution to the parameter space of q for this

Table 1
Logarithmic Odd Ratios ($\ln \mathcal{O}$) and Bayes Factors ($\ln \mathcal{B}$) of the CHE Prior and the SMT Prior Compared to the CEE Prior

Name	CHE $\ln \mathcal{O}(\ln \mathcal{B})$	SMT $\ln \mathcal{O}(\ln \mathcal{B})$
GW190517_055101	3.4(4.2)	−8.7(−9.3)
GW190805_211137	2.4(3.1)	−0.7(−1.4)
GW190620_030421	1.4(2.1)	−2.7(−3.3)
GW170729	1.2(1.9)	−1.4(−2.1)
GW200216_220804	0.5(1.2)	0.9(0.2)
GW190719_215514	−0.6(0.1)	0.3(−0.4)
GW190527_092055	−2.1(−1.4)	1.3(0.6)
GW200128_022011	−2.1(−1.4)	2.3(1.6)
GW170823	−3.2(−2.5)	1.8(1.1)
GW190513_205428	−3.4(−2.7)	0.7(0.0)
GW190727_060333	−3.5(−2.7)	1.9(1.2)
GW190828_063405	−4.3(−3.6)	0.7(0.1)
GW170809	−6.0(−5.2)	1.7(1.0)
GW190630_185205	−7.1(−6.3)	1.0(0.4)
GW200224_222234	−7.4(−6.7)	2.4(1.8)
GW200129_065458	−12.2(−11.5)	1.3(0.6)
GW170814	−14.9(−14.2)	2.0(1.3)
GW190925_232845	−16.3(−15.6)	−4.0(−4.7)
GW191103_012549	−18.6(−17.9)	−16.1(−16.8)
GW190930_133541	−20.0(−19.3)	−18.5(−19.2)
GW200316_215756	−21.8(−21.1)	−20.9(−21.6)
GW151226	−41.6(−40.9)	−40.3(−41.0)
GW190728_064510	−46.9(−46.1)	−48.3(−48.9)
GW191129_134029	−57.6(−56.9)	−18.8(−19.5)
GW191204_171526	−106.8(−106.0)	−21.8(−22.5)
GW191216_213338	−124.4(−123.7)	−127.4(−128.1)

event. Other events, GW170729, GW190620_030421, and GW190805_211137 have moderate support on the CHE prior.

In Figure 3, we show posterior distributions of the six events with $\mathcal{O} > 1/3$ on the CHE channel to illustrate the impact of the prior. Similar to GW190517_055101, the mass ratio distributions of the other events all peak at $q \gtrsim 0.8$, and their posterior supports drop rapidly toward the lower edge of the prior. On the other hand, by comparing the distributions in Figure 3 with the priors as shown in Figure 1, one can observe that our choices of prior strongly affect the posterior distribution of χ_i and q compared to the LVK's default prior. We also show the results for the eight events that most favor ($\mathcal{O} > 3$) the SMT hypothesis in Appendix.

With the Bayes factors and posterior distributions of each event, one can derive the astrophysical merger rate density ($\mathcal{R}0$) in the local universe ($z = 0$) for each channel. Following the method described in Kim et al. (2003) and Abbott et al. (2016a), we calculate the "event-based" merger rate density for each event. The method treats every single event as a unique subclass of BBHs and calculates their merger rate density separately. Then, the total event rate is the sum of the individual rates. The Poisson fluctuation and the uncertainties of the parameters inferred with each prior are taken into account in the calculation (see Section 6 and Appendix C in Abbott et al. 2016a for details). The injection provided by Abbott et al. (2021a) is utilized to estimate the instruments' sensitivity for searching mergers similar to each event. We consider an evolving merger rate density with the form $\mathcal{R}_i = \mathcal{R}0_i(1+z)^{2.7}$, where $\mathcal{R}0_i$ is the local merger rate density for the BBHs with properties similar to the ith event in our sample. Adopting a uniform prior for the local merger rate density, we obtain the posterior distributions for $\mathcal{R}0_i$ of different events. Second, we randomly draw a value from the $\mathcal{R}0_i$ posterior distribution for each event, and multiply each of them by a weight decided by the events' $\mathcal{B}$ s (for a particular event, the sum of weights for the three channels is 1). Then, we sum over these reweighted values to obtain the overall $\mathcal{R}0$ s. By repeating the above steps 50,000 times, we numerically derived the probability distributions for $\mathcal{R}0$ of each channel. Since our selected events make up a subset of the entire catalog, the derived results can only be regarded as the lower limits for $\mathcal{R}0$. By integrating the probability distributions, the lower limits are $11.45\,\mathrm{Gpc^{-3}\,yr^{-1}}$, $0.18\,\mathrm{Gpc^{-3}\,yr^{-1}}$, and $0.63\,\mathrm{Gpc^{-3}\,yr^{-1}}$ at 90% credible level for the CEE, CHE, and SMT channels, respectively.

4. Conclusions and Discussion

Although significant progress in gravitational-wave astrophysics today has been made in the past several years, the origin of the BBHs remains an open scientific question. In the modeling for the origin of BBHs, isolated binary evolution has been considered as a leading formation channel, in which the CHE channel was recently found to play an essential role in contributing to the whole population of BBH mergers (Marchant et al. 2016; Mandel & de Mink 2016; de Mink & Mandel 2016; du Buisson et al. 2020; Zevin et al. 2021; Riley et al. 2021; Bavera et al. 2022c). However, none of these events have been reported with a significantly high evidence for being formed through this channel.

In this work, we search for candidates of merging BBHs originating from the CHE channel in GWTC-3, using Bayesian inference with astrophysically predicted priors. Assuming GWTC-3 events originated from isolated binary evolution, we reanalyze a subsample of events using a suite of state-of-the-art models (du Buisson et al. 2020; Bavera et al. 2021) as released by Zevin et al. (2021). After performing the Bayesian inference for the target events, we report strong evidence ($\ln \mathcal{O} = 3.4$) for GW190517_055101 being formed through the CHE channel. Under the assumption that the selected events in our subsample are all formed through one of the three channels considered in this work, we thus obtain the lower limits on the local merger rate density of these channels, $11.45\,\mathrm{Gpc^{-3}\,yr^{-1}}$ (CEE), $0.18\,\mathrm{Gpc^{-3}\,yr^{-1}}$ (CHE), and $0.63\,\mathrm{Gpc^{-3}\,yr^{-1}}$ (SMT) at 90% credible level, respectively.

It is still a challenge to quantitatively predict the BBHs' properties due to uncertain physical processes involved in the single and/or binary evolution of massive stars (Belczynski et al. 2022). The upper limit of the stellar-mass BH predicted by (pulsational) pair-instability supernovae (e.g., Woosley 2017; Marchant et al. 2019; Farmer et al. 2019) is still uncertain. Additionally, the models we adopt in this work assume efficient AM transport (Spruit 2002; Fuller & Ma 2019) in the progenitor massive stars, which leads to forming first-born BHs with negligible spins (Qin et al. 2018; Fuller & Ma 2019). We note that BHs could obtain a slightly large spin ($\sim$0.1) depending on the physics accounted for in the stellar models (Belczynski et al. 2020). Schürmann et al. (2022) recently showed new supports for efficient internal AM transport for studying the spins of stripped B-type stars. However, this efficient mechanism could be challenged (Qin et al. 2022b) with the detection of GW190403_051519 (Abbott et al. 2021e), under the assumption that this merger event was formed through the CEE channel. In the upcoming O4

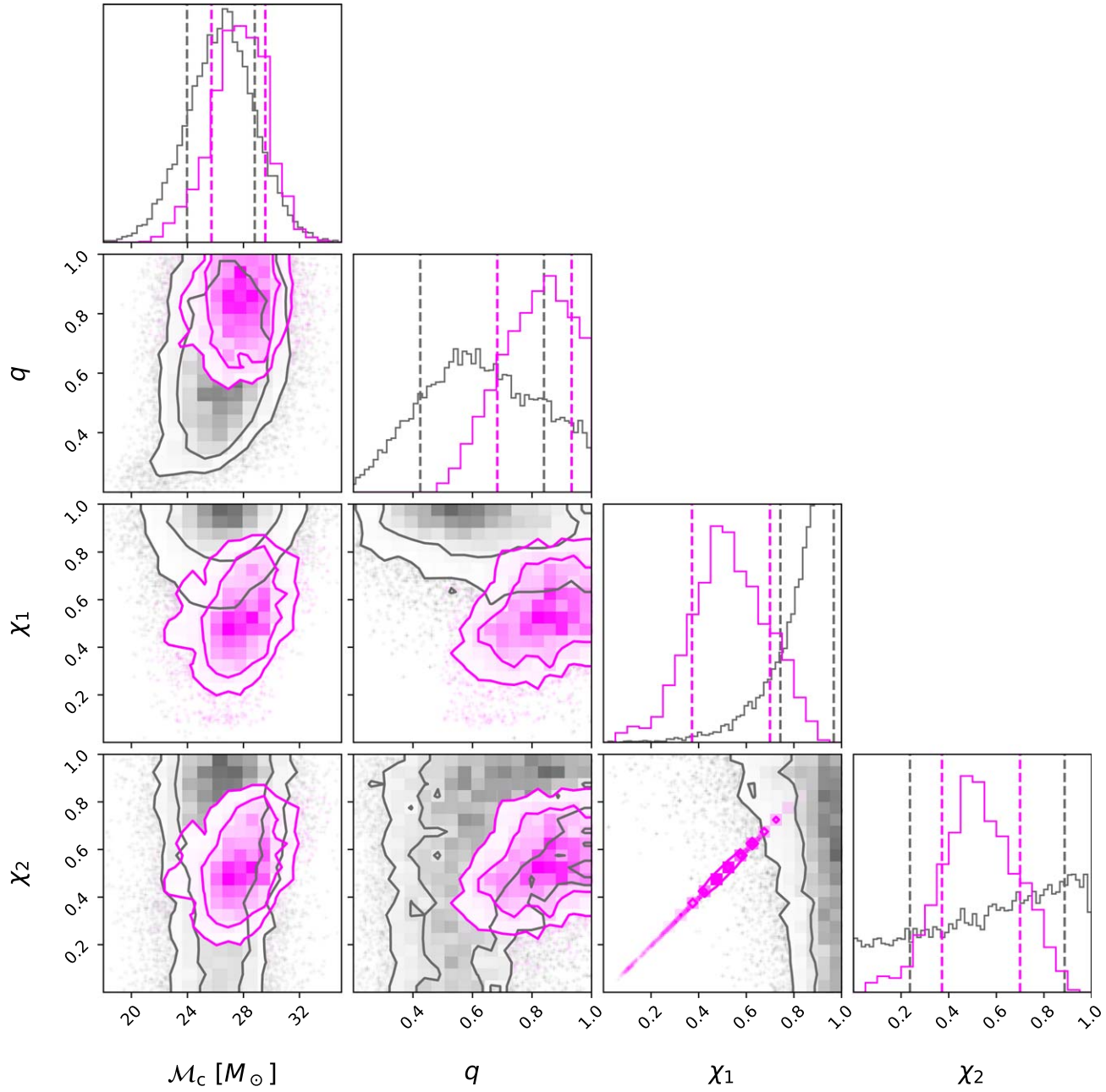

Figure 2. The posterior distributions for GW190517_055101 inferred by LVK's default prior (gray) and the CHE prior (magenta). The inner and outer solid circles in the 2D plots mark the 68% and 90% credible regions, respectively.

Observing run of the LVK, more events like GW190517_055101 are expected to be detected, and hence, this will allow the unraveling of the population properties of BBHs predicted by the CHE channel and further put stronger constraints on the physical processes in the evolution of massive stars in close binary systems.

We thank Ilya Mandel for helpful comments on the manuscript. We thank Zi-Qing Xia for useful discussion. Y. Q. acknowledges the support from the Doctoral research start-up funding of Anhui Normal University. Y.Z.W. is supported by NSFC (grant No. 12203101). This work was supported by the National Natural Science Foundation of China (NSFC, grant Nos. 11863003, 12003002, 12103003, 12173010, 12192220, 12192221) and by the Natural Science Foundation of Universities in Anhui Province (grant No. KJ2021A0106). S.S.B. is supported by the Swiss National Science Foundation (project number PP00P2_176868). G.M. has received funding from the European Research Council (ERC) under the European Union's Horizon 2020 research and innovation program (grant agreement No. 833925, project STAREX). D. M.W. is supported by NSFC (Nos. 12073080, 11933010, 11921003) and the Chinese Academy of Sciences via the Key Research Program of Frontier Sciences (No. QYZDJSSW-SYS024).

All figures are made with the free Python module Matplotlib (Hunter 2007). We would also like to thank all of the essential workers who put their health at risk during the COVID-19 pandemic, without whom we would not have been able to complete this work.

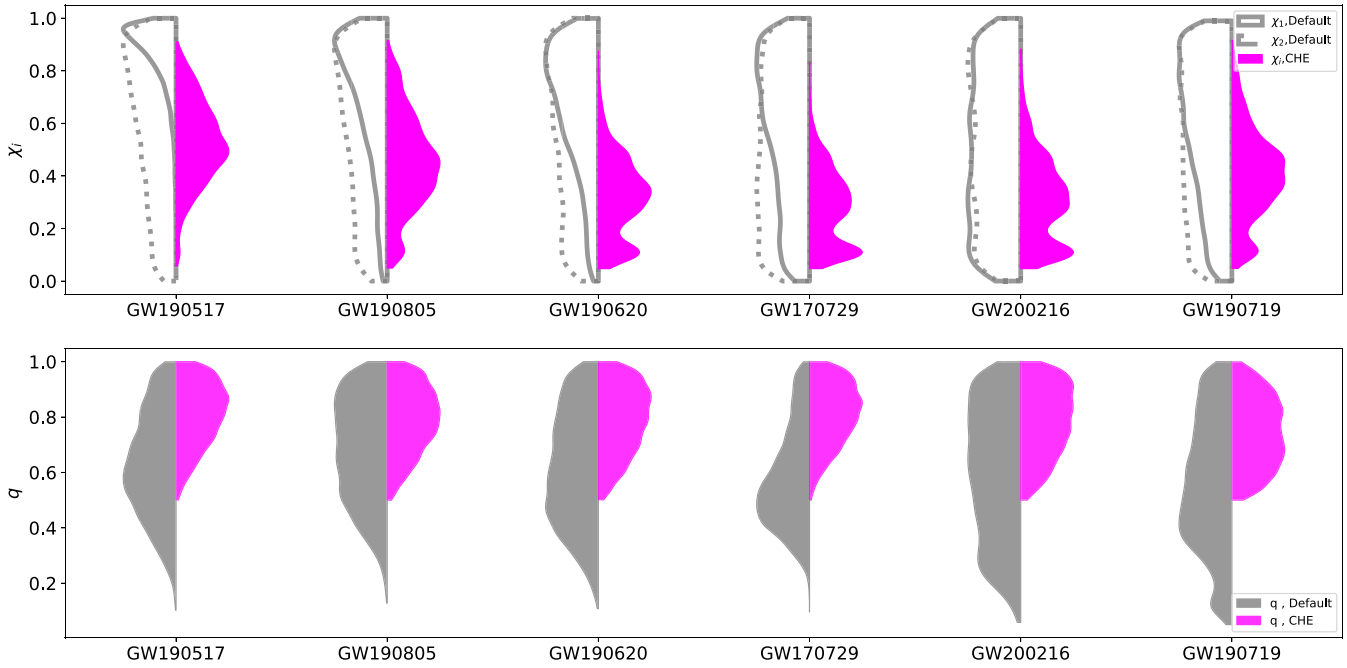

Figure 3. Violin plot showing marginal posterior distributions of individual spins (upper panel) and mass ratios (lower panel) inferred with LVK's default prior and the CHE prior. These selected events have odd ratios larger than 1/3 for the CHE channel. For brevity, we omit the suffix of the event name.

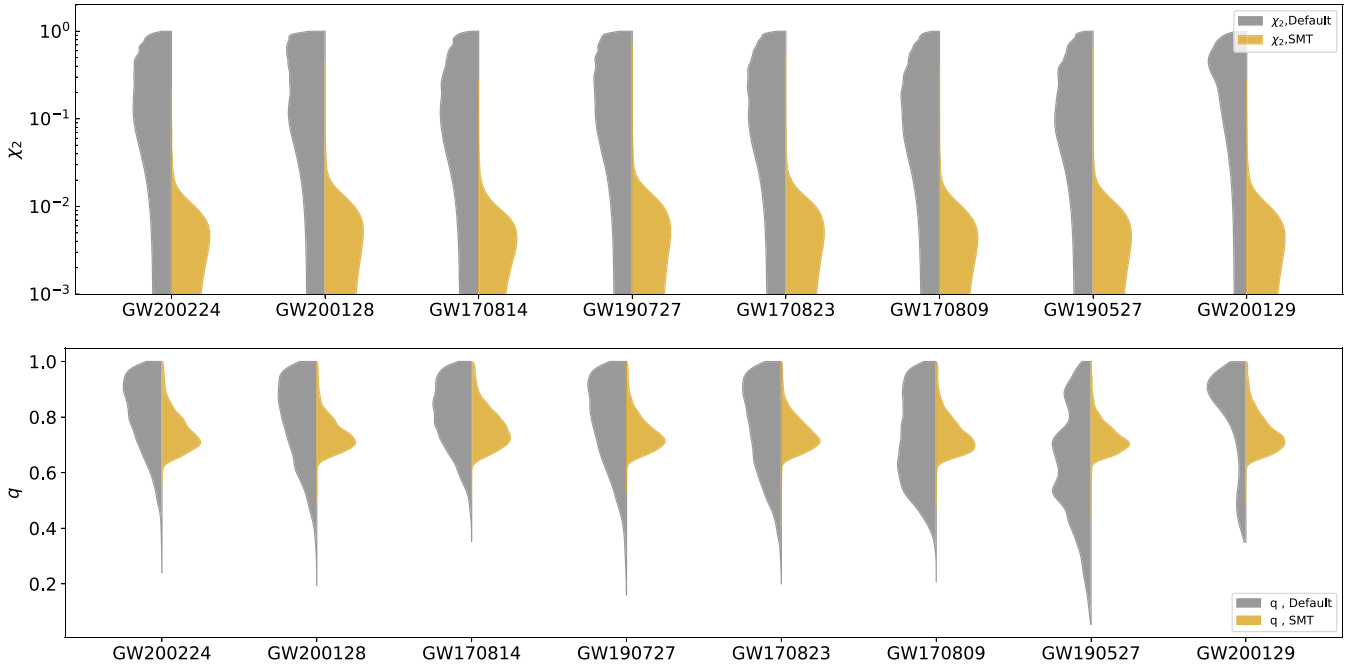

Figure 4. The same as Figure 3, but for the results inferred with the SMT prior. The selected events have odd ratios larger than three for the SMT channel.

Appendix
Supplementary Figure (Figure 4)

ORCID iDs

Ying Qin https://orcid.org/0000-0002-2956-8367
Yuan-Zhu Wang https://orcid.org/0000-0001-9626-9319
Simone S. Bavera https://orcid.org/0000-0002-3439-0321
Shichao Wu https://orcid.org/0000-0002-9188-5435
Georges Meynet https://orcid.org/0000-0001-6181-1323
Yi-Ying Wang https://orcid.org/0000-0003-1215-6443
Rui-Chong Hu https://orcid.org/0000-0002-6442-7850
Jin-Ping Zhu https://orcid.org/0000-0002-9195-4904
Dong-Hong Wu https://orcid.org/0000-0001-9424-3721
Xin-Wen Shu https://orcid.org/0000-0002-7020-4290
Fang-Kun Peng https://orcid.org/0000-0001-7171-5132
Han-Feng Song https://orcid.org/0000-0002-5484-6090
Da-Ming Wei https://orcid.org/0000-0002-9758-5476

References

Abbott, B. P., Abbott, R., Abbott, T. D., et al. 2016a, PhRvX, 6, 041015
Abbott, B. P., Abbott, R., Abbott, T. D., et al. 2016b, PhRvL, 116, 061102
Abbott, R., Abbott, T. D., Abraham, S., et al. 2020, PhRvD, 102, 043015

Abbott, R., Abbott, T. D., Abraham, S., et al. 2021c, PhRvX, 11, 021053
Abbott, R., Abbott, T. D., Abraham, S., et al. 2021d, ApJL, 913, L7
Abbott, R., Abbott, T. D., Acernese, F., et al. 2020b, arXiv:2111.03606
Abbott, R., Abbott, T. D., Acernese, F., et al. 2021a, arXiv:2111.03634
Abbott, R., Abbott, T. D., Acernese, F., et al. 2021e, arXiv:2108.01045
Adamcewicz, C., & Thrane, E. 2022, MNRAS, 517, 3928
Ashton, G., Hübner, M., Lasky, P. D., et al. 2019, Bilby: Bayesian Inference Library, Astrophysics Source Code Library, ascl:1901.011
Bavera, S. S., Fishbach, M., Zevin, M., Zapartas, E., & Fragos, T. 2022a, A&A, 665, A59
Bavera, S. S., Fragos, T., Qin, Y., et al. 2020, A&A, 635, A97
Bavera, S. S., Fragos, T., Zapartas, E., et al. 2022c, A&A, 657, L8
Bavera, S. S., Fragos, T., Zevin, M., et al. 2021, A&A, 647, A153
Bavera, S. S., Franciolini, G., Cusin, G., et al. 2022b, A&A, 660, A26
Belczynski, K., Holz, D. E., Bulik, T., & O'Shaughnessy, R. 2016, Natur, 534, 512
Belczynski, K., Kalogera, V., & Bulik, T. 2002, ApJ, 572, 407
Belczynski, K., Klencki, J., Fields, C. E., et al. 2020, A&A, 636, A104
Belczynski, K., Romagnolo, A., Olejak, A., et al. 2022, ApJ, 925, 69
Bethe, H. A., & Brown, G. E. 1998, ApJ, 506, 780
Bouffanais, Y., Mapelli, M., Santoliquido, F., et al. 2021, MNRAS, 507, 5224
Broekgaarden, F. S., Berger, E., Stevenson, S., et al. 2022, MNRAS, 516, 5737
Callister, T. A., Haster, C.-J., Ng, K. K. Y., Vitale, S., & Farr, W. M. 2021, ApJL, 922, L5
Cantiello, M., Yoon, S. C., Langer, N., & Livio, M. 2007, A&A, 465, L29
Chia, H. S., Olsen, S., Roulet, J., et al. 2022, PhRvD, 106, 024009
Damour, T. 2001, PhRvD, 64, 124013
de Mink, S. E., Cantiello, M., Langer, N., et al. 2009, A&A, 497, 243
de Mink, S. E., Langer, N., Izzard, R. G., Sana, H., & de Koter, A. 2013, ApJ, 764, 166
de Mink, S. E., & Mandel, I. 2016, MNRAS, 460, 3545
du Buisson, L., Marchant, P., Podsiadlowski, P., et al. 2020, MNRAS, 499, 5941
Estellés, H., Husa, S., Colleoni, M., et al. 2022, ApJ, 924, 79
Farmer, R., Renzo, M., de Mink, S. E., Marchant, P., & Justham, S. 2019, ApJ, 887, 53
Farr, B., Holz, D. E., & Farr, W. M. 2018, ApJL, 854, L9
Farr, W. M., Stevenson, S., Miller, M. C., et al. 2017, Natur, 548, 426
Fishbach, M., & Holz, D. E. 2020, ApJL, 904, L26
Fragione, G., & Kocsis, B. 2018, PhRvL, 121, 161103
Franciolini, G., Baibhav, V., De Luca, V., et al. 2022, PhRvD, 105, 083526
Fuller, J., & Lu, W. 2022, MNRAS, 511, 3951
Fuller, J., & Ma, L. 2019, ApJL, 881, L1
Fuller, J., Piro, A. L., & Jermyn, A. S. 2019, MNRAS, 485, 3661
Galaudage, S., Talbot, C., Nagar, T., et al. 2021, ApJL, 921, L15
Ghodla, S., Eldridge, J. J., Stanway, E. R., & Stevance, H. F. 2023, MNRAS, 518, 860
Gupta, P., Suzuki, H., Okawa, H., & Maeda, K.-i. 2020, PhRvD, 101, 104053
Hoy, C., Mills, C., & Fairhurst, S. 2022, PhRvD, 106, 023019
Hunter, J. D. 2007, CSE, 9, 90
Inayoshi, K., Hirai, R., Kinugawa, T., & Hotokezaka, K. 2017, MNRAS, 468, 5020
Islam, T., Field, S. E., Haster, C.-J., & Smith, R. 2021, PhRvD, 103, 104027
Kalogera, V., Belczynski, K., Kim, C., O'Shaughnessy, R., & Willems, B. 2007, PhR, 442, 75
Kim, C., Kalogera, V., & Lorimer, D. R. 2003, ApJ, 584, 985
Lipunov, V. M., Postnov, K. A., & Prokhorov, M. E. 1997, MNRAS, 288, 245
Maeder, A. 1987, A&A, 178, 159
Mandel, I., & Broekgaarden, F. S. 2022, LRR, 25, 1
Mandel, I., & de Mink, S. E. 2016, MNRAS, 458, 2634
Mandel, I., & Farmer, A. 2022, PhR, 955, 1
Mandel, I., & Fragos, T. 2020, ApJL, 895, L28
Mandel, I., & Smith, R. J. E. 2021, ApJL, 922, L14
Mapelli, M. 2021, in Handbook of Gravitational Wave Astronomy, ed. C. Bambi, S. Katsanevas, & K. D. Kokkotas (Berlin: Springer)
Mapelli, M., Bouffanais, Y., Santoliquido, F., Arca Sedda, M., & Artale, M. C. 2022, MNRAS, 511, 5797
Marchant, P., Langer, N., Podsiadlowski, P., et al. 2017, A&A, 604, A55
Marchant, P., Langer, N., Podsiadlowski, P., Tauris, T. M., & Moriya, T. J. 2016, A&A, 588, A50
Marchant, P., Renzo, M., Farmer, R., et al. 2019, ApJ, 882, 36
Martins, F., Depagne, E., Russeil, D., & Mahy, L. 2013, A&A, 554, A23
McKernan, B., Ford, K. E. S., Bellovary, J., et al. 2018, ApJ, 866, 66
Neijssel, C. J., Vigna-Gómez, A., Stevenson, S., et al. 2019, MNRAS, 490, 3740
Olejak, A., & Belczynski, K. 2021, ApJL, 921, L2
Payne, E., Hourihane, S., Golomb, J., et al. 2022, PhRvD, 106, 104017
Pratten, G., García-Quirós, C., Colleoni, M., et al. 2021, PhRvD, 103, 104056
Qin, Y., Fragos, T., Meynet, G., et al. 2018, A&A, 616, A28
Qin, Y., Marchant, P., Fragos, T., Meynet, G., & Kalogera, V. 2019, ApJL, 870, L18
Qin, Y., Shu, X., Yi, S., & Wang, Y.-Z. 2022a, RAA, 22, 035023
Qin, Y., Wang, Y.-Z., Wu, D.-H., Meynet, G., & Song, H. 2022b, ApJ, 924, 129
Riley, J., Mandel, I., Marchant, P., et al. 2021, MNRAS, 505, 663
Rodriguez, C. L., & Antonini, F. 2018, ApJ, 863, 7
Rodriguez, C. L., Morscher, M., Pattabiraman, B., et al. 2015, PhRvL, 115, 051101
Rodriguez, C. L., Zevin, M., Pankow, C., Kalogera, V., & Rasio, F. A. 2016, ApJ, 832, L2
Roulet, J., Chia, H. S., Olsen, S., et al. 2021, PhRvD, 104, 083010
Sana, H., de Mink, S. E., de Koter, A., et al. 2012, Sci, 337, 444
Schürmann, C., Langer, N., Xu, X., & Wang, C. 2022, A&A, 667, A122
Shao, Y., & Li, X.-D. 2022, ApJ, 930, 26
Silsbee, K., & Tremaine, S. 2017, ApJ, 836, 39
Stevenson, S., Berry, C. P. L., & Mandel, I. 2017, MNRAS, 471, 2801
Song, H. F., Meynet, G., Maeder, A., Ekström, S., & Eggenberger, P. 2016, A&A, 585, A120
Speagle, J. S. 2020, MNRAS, 493, 3132
Spruit, H. C. 2002, A&A, 381, 923
Tagawa, H., Haiman, Z., Bartos, I., & Kocsis, B. 2020, ApJ, 899, 26
Talbot, C., & Thrane, E. 2017, PhRvD, 96, 023012
Thrane, E., & Talbot, C. 2019, PASA, 36, e010
Toonen, S., Portegies Zwart, S., Hamers, A. S., & Bandopadhyay, D. 2020, A&A, 640, A16
Tutukov, A. V., & Yungelson, L. R. 1993, MNRAS, 260, 675
Vajpeyi, A., Smith, R., & Thrane, E. 2022, arXiv:2203.13406
van den Heuvel, E. P. J., Portegies Zwart, S. F., & de Mink, S. E. 2017, MNRAS, 471, 4256
Vink, J. S., de Koter, A., & Lamers, H. J. G. L. M. 2001, A&A, 369, 574
Vitale, S., Biscoveanu, S., & Talbot, C. 2022, A&A, 668, L2
Vitale, S., Lynch, R., Sturani, R., & Graff, P. 2017, CQGra, 34, 03LT01
Wong, K. W. K., Breivik, K., Farr, W. M., & Luger, R. 2022, arXiv:2206.04062
Wong, K. W. K., Breivik, K., Kremer, K., & Callister, T. 2021, PhRvD, 103, 083021
Woosley, S. E. 2017, ApJ, 836, 244
Zevin, M. 2021, ApJ, 910, 152
Zevin, M., & Bavera, S. S. 2022, ApJ, 933, 86
Zevin, M., Bavera, S. S., Berry, C. P. L., et al. 2021, ApJ, 910, 152
Zevin, M., Berry, C. P. L., Coughlin, S., Chatziioannou, K., & Vitale, S. 2020, ApJL, 899, L17